

536  
UNCLASSIFIED

NRL Report 5683

# IDEAL LIMITING

## PART 1 - THE EFFECT OF IDEAL LIMITING ON SIGNALS AND ON NOISE

S. F. George and J. W. Wood

Radar Division

October 2, 1961



U. S. NAVAL RESEARCH LABORATORY  
Washington, D.C.

Current Reports in This Series

"Part 1 - The Effect of Ideal Limiting on Signals and on Noise," S. F. George and J. W. Wood, NRL Report 5683, September 1961

"Part 2 - The Operation of an Ideal Limiter on Signals Imbedded in Noise," S. F. George and J. W. Wood, NRL Report 5684, September 1961

## CONTENTS

Abstract	ii
Problem Status	ii
Authorization	ii
INTRODUCTION	1
THE IDEAL LIMITER	1
PART I. SIGNALS ALONE	2
Single Sine-Wave Input	2
Input Consisting of Two Sine Waves	4
PART II. NOISE ALONE	8
Input of Band-Limited White Noise	10
White Noise Through Single-Tuned Circuit	12
Bandpass Filter	13
REFERENCES	18
APPENDIX A - Evaluation of Contour Integral	19
APPENDIX B - Calculation for the Case of Band-Limited White Noise	21

## ABSTRACT

The effect of hard clipping or ideal limiting on sine-wave signals and on shaped, Gaussian-noise inputs is considered. For a single sine wave, the limiter reproduces the fundamental frequency and creates odd harmonics of rapidly decreasing relative power. For two sine-wave inputs of equal amplitudes, the limiter generates arrays of beat frequencies centered symmetrically about the two input frequencies and their shifted odd harmonics. If the two inputs are of unequal amplitude, the stronger signal suppresses the weaker. On shaped, wide-band Gaussian noise, the limiter tends to broaden the high-frequency end of the spectrum slightly and to produce a flat, low-frequency, random-noise response.

## PROBLEM STATUS

The work reported applies to problems involved in the analog-digital conversion of data for the U. S. Naval Space Surveillance System. This is the first of two reports on this phase of the problem; work on other phases continues.

## AUTHORIZATION

NRL Problem RO2-82  
ARPA Order 7-58

Manuscript submitted July 17, 1961.

## IDEAL LIMITING

### PART 1 - THE EFFECT OF IDEAL LIMITING ON SIGNALS AND ON NOISE

#### INTRODUCTION

Although the general theory for nonlinear devices has been exhaustively studied (1) and the spectral changes in clipped, rectangular-shaped noise have been worked out (2-4), the need still remained for a concise engineering examination of the results of limiting signals and the effect of limiting more practical shapes of filtered noise. The purpose of this work is to determine what a limiter does to two sine waves of different frequencies and amplitudes and how shaped, Gaussian noise is altered by clipping. The general method used will follow Davenport and Root (1a) for handling nonlinear devices. A second report will treat the more practical case of sine-wave signals embedded in Gaussian noise.

#### THE IDEAL LIMITER

A limiter is a device which truncates the amplitude of a signal at a given value. By setting this amplitude very close to zero and then amplifying the resulting signal an ideal limiter can be approximated (Fig. 1). In terms of the amplification characteristics, an ideal limiter is approached as  $\epsilon$  tends to zero and as the actual curve approaches its asymptotes (Fig. 2).

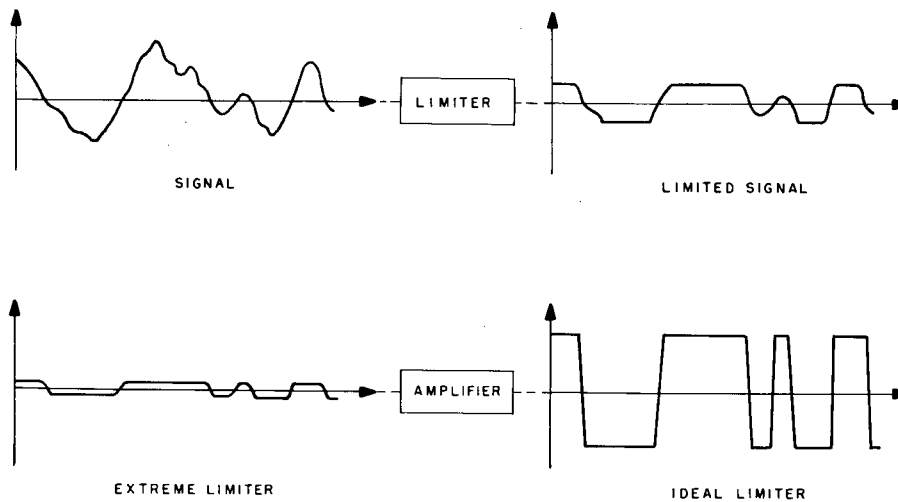


Fig. 1 - Illustration of limited signal  
and ideal limiter

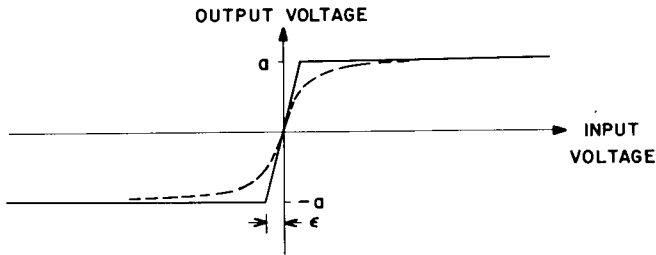


Fig. 2 - Output voltage vs input voltage for a limiter. Solid lines represent the ideal case, dotted line a possible limiter characteristic.

## PART I. SIGNALS ALONE

### Single Sine-Wave Input

The general approach to the solution of this problem is through the Laplace transform. Let  $g(x)$  be the transfer characteristic of the limiter and  $f(\omega)$  be the transfer function or bilateral Laplace transform of  $g(x)$ . The bilateral transform must be used since  $x$  is not restricted in range to  $x > 0$  as is the case in the more conventional unilateral Laplace transform. We then have

$$f(\omega) = \int_{-\infty}^{\infty} g(x) e^{-\omega x} dx \quad (1)$$

and

$$g(x) = \frac{1}{2\pi j} \int_{u-j\infty}^{u+j\infty} f(\omega) e^{x\omega} d\omega \quad (2)$$

where the value of  $u$  in the contour integral must be properly defined.

In the case at hand, that of an ideal limiter ( $\epsilon = 0$ ), we can define  $g(x)$  as follows:

$$\begin{aligned} g(x) &= +a, & x > 0 \\ g(x) &= 0, & x = 0 \\ g(x) &= -a, & x < 0 \end{aligned} \quad (3)$$

so that we have a corresponding separation of  $f(\omega)$  into  $f_+(\omega)$  where  $x > 0$  and  $f_-(\omega)$  where  $x < 0$  with different regions of convergence. Here

$$f_+(\omega) = \int_0^{\infty} a e^{-\omega x} dx, \quad \text{Re}(\omega) > 0 \quad (4)$$

where, for the inverse transformation, the contour of integration over  $f_+(\omega)$ ,  $C_+$ , must be a line  $\omega = \epsilon + jv$  with  $\epsilon > 0$  and  $-\infty < v < \infty$ . Also,

$$f_-(\omega) = \int_{-\infty}^0 (-a) e^{-\omega x} dx, \quad \text{Re}(\omega) < 0 \quad (5)$$

where  $C_-$  must be a line  $\omega = -\epsilon + jv$  with  $\epsilon > 0$  and  $-\infty < v < \infty$ . Evaluation of these integrals yields

$$f_+(\omega) = f_-(\omega) = \frac{a}{\omega}. \quad (6)$$

Now for the input to the limiter let us use

$$x \equiv x(t) = V \cos \omega_1 t \equiv V \cos \theta,$$

and redefine  $g(x)$  by  $g(x) = g[x(t)] \equiv y(t)$ , where we will assume  $v$  to be constant and  $\theta = \omega_1 t$ . The output  $y(t)$  of the limiter will then be

$$y(t) = \frac{a}{2\pi j} \int_{\epsilon-j\infty}^{\epsilon+j\infty} \frac{e^{\omega V \cos \theta}}{\omega} d\omega + \frac{a}{2\pi j} \int_{-\epsilon-j\infty}^{-\epsilon+j\infty} \frac{e^{\omega V \cos \theta}}{\omega} d\omega. \quad (7)$$

This reduces to

$$y = \frac{a}{2\pi j} \int_{\epsilon-j\infty}^{\epsilon+j\infty} \frac{e^{\omega V \cos \theta} - e^{-\omega V \cos \theta}}{\omega} d\omega. \quad (8)$$

By the Jacobi-Anger formula,

$$e^z \cos \theta = \sum_{m=0}^{\infty} \mathcal{E}_m I_m(z) \cos m\theta$$

where  $\mathcal{E}_m$  is the Neumann factor,  $\mathcal{E}_0 = 1$ ,  $\mathcal{E}_m = 2$  ( $m > 0$ ), and  $I_m(z)$  is the modified Bessel function of the first kind. Whence,

$$y = \frac{a}{2\pi j} \sum_{m=0}^{\infty} \mathcal{E}_m \cos m\theta \int_{\epsilon-j\infty}^{\epsilon+j\infty} \left[ \frac{I_m(\omega V)}{\omega} - \frac{I_m(-\omega V)}{\omega} \right] d\omega. \quad (9)$$

Now  $I_m(-z) = (-1)^m I_m(z)$ ; therefore,

$$y = a \sum_{m=0}^{\infty} \left[ 1 - (-1)^m \right] \mathcal{E}_m \cos m\theta \frac{1}{2\pi j} \int_{\delta-j\infty}^{\delta+j\infty} \frac{I_m(z)}{z} dz, \quad (10)$$

where we have let  $z = \omega V$  and  $\delta = \epsilon V$ . Integrals of the form of Eq. (10) have been evaluated by Davenport (1b) with the result

$$I = \frac{1}{2\pi j} \int_{\delta-j\infty}^{\delta+j\infty} \frac{I_m(z)}{z} dz = \frac{1}{2\pi j} \int_{-j\infty}^{j\infty} \frac{I_m(z)}{z} dz. \quad (11)$$

Using the relation  $I_m(jx) = j^m J_m(x)$  we reduce this to

$$I = \frac{j^m}{2\pi j} \int_{-\infty}^{\infty} \frac{J_m(x)}{x} dx,$$

which is easily seen to yield

$$I = \frac{j^m}{2\pi j} [1 - (-1)^m] \int_0^{\infty} \frac{J_m(x)}{x} dx. \quad (12)$$

Now the expression  $j^m [1 - (-1)^m]$  yields zero for all even values of  $m$  and yields  $\pm 2j$  for odd values. This can be written as

$$j^m [1 - (-1)^m] = 2j \sin \frac{m\pi}{2}.$$

Also, the integral in Eq. (12) can be evaluated by using Weber's infinite integral (5a) given as

$$\int_0^{\infty} \frac{J_{\nu}(t)}{t^{\nu-\mu+1}} dt = \frac{\Gamma\left(\frac{\mu}{2}\right)}{2^{\nu-\mu+1} \Gamma\left(\nu - \frac{\mu}{2} + 1\right)}. \quad (13)$$

Here, if we let  $\nu = m$ ,  $t = x$ , and  $\mu = m$ , we have the integral of Eq. (12); thus,

$$\int_0^{\infty} \frac{J_m(x)}{x} dx = \frac{\Gamma\left(\frac{m}{2}\right)}{2\Gamma\left(\frac{m}{2} + 1\right)} = \frac{1}{m}. \quad (14)$$

Finally, then, we have

$$I = \frac{1}{m\pi} \sin \frac{m\pi}{2}. \quad (15)$$

The final output in Eq. (10) is

$$y = \frac{4a}{\pi} \sum_{m=1}^{\infty} \frac{1}{m} \sin \frac{m\pi}{2} \cos m\omega_1 t. \quad (16)$$

This series expansion, which of course corresponds to the harmonic content of a square wave, is plotted in Fig. 3. Here, the relative power content at the discrete frequencies is shown versus frequency, based on an input frequency of 1 kc and a clipping level of unity.

#### Input Consisting of Two Sine Waves

To determine the limiter output for the case where the input consists of two sine waves of different frequencies, the same general theory applies. Here, however,

$$x = x(t) = V_1 \cos \omega_1 t + V_2 \cos \omega_2 t = V_1 \cos \theta_1 + V_2 \cos \theta_2 \quad (17)$$

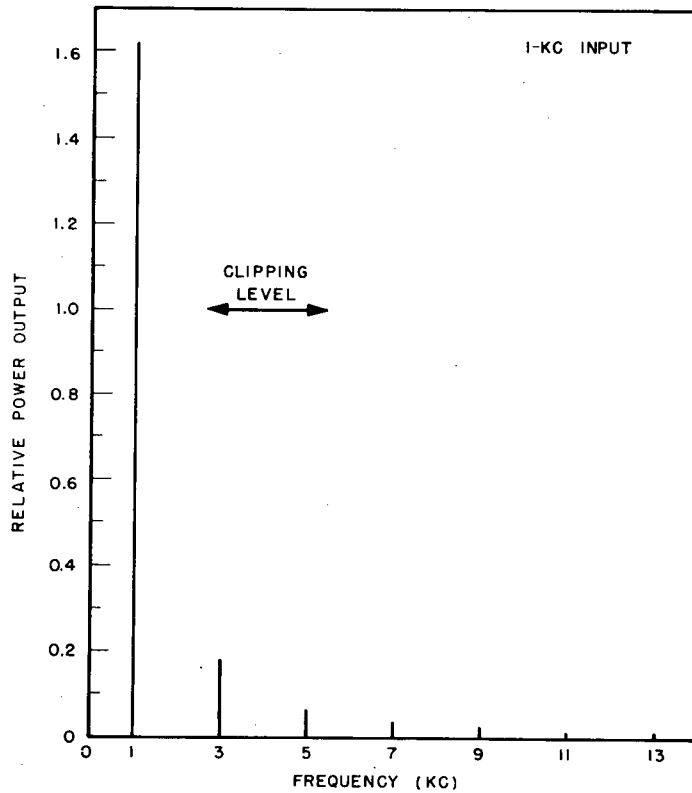


Fig. 3 - Output power spectrum of ideal limiter for a single sine-wave input

where  $V_1 = V_2$  only as a special case. Substituting this expression in Eq. (8), the limiter output becomes

$$y = \frac{a}{2\pi j} \int_{\epsilon-j\infty}^{\epsilon+j\infty} \frac{d\omega}{\omega} \left\{ e^{\omega(V_1 \cos \theta_1 + V_2 \cos \theta_2)} - e^{-\omega(V_1 \cos \theta_1 + V_2 \cos \theta_2)} \right\} \quad (18)$$

Again applying the Jacobi-Anger formula, this expression reduces to

$$y = a \sum_{m=0}^{\infty} \sum_{n=0}^{\infty} [1 - (-1)^{m+n}] \mathcal{E}_m \mathcal{E}_n \cos m\theta_1 \cos n\theta_2 \frac{1}{2\pi j} \int_{\epsilon-j\infty}^{\epsilon+j\infty} \frac{I_m(\omega V_1) I_n(\omega V_2)}{\omega} d\omega \quad (19)$$

The problem then is to evaluate the contour integral.

It is shown in Appendix A that

$$\int_{\epsilon-j\infty}^{\epsilon+j\infty} \frac{I_m(\omega V_1) I_n(\omega V_2)}{\omega} d\omega = j^{m+n} [1 - (-1)^{m+n}] \int_0^{\infty} \frac{J_m(xV_1) J_n(xV_2)}{x} dx \quad (20)$$

In terms of Eq. (20), the output from Eq. (19) then becomes

$$y = \frac{a}{\pi} \sum_{m=0}^{\infty} \sum_{n=0}^{\infty} \mathcal{E}_m \mathcal{E}_n [1 - (-1)^{m+n}] \sin \frac{(m+n)\pi}{2} \cos m\omega_1 t \cos n\omega_2 t \int_0^{\infty} \frac{J_m(xV_1) J_n(xV_2)}{x} dx. \quad (21)$$

1. Special Case:  $V_1 = V_2 = V$ .

The integral in Eq. (21) becomes a special case of the Weber-Schafheitlin integral (5b),

$$\int_0^{\infty} J_{\mu}(at) J_{\nu}(at) \frac{dt}{t} = \frac{2}{\pi} \frac{\sin \frac{1}{2}(\nu - \mu)\pi}{\nu^2 - \mu^2} \quad (22)$$

where  $a = V_1 = V_2$ . Using this in Eq. (21) we obtain the final result

$$y = \frac{a}{\pi^2} \sum_{m=0}^{\infty} \sum_{n=0}^{\infty} \mathcal{E}_m \mathcal{E}_n [1 - (-1)^{m+n}] \frac{1}{m^2 - n^2} \sin \frac{(m+n)\pi}{2} \sin \frac{(m-n)\pi}{2} \\ \times \{ \cos (m\omega_1 + n\omega_2)t + \cos (m\omega_1 - n\omega_2)t \}. \quad (23)$$

As can be seen, terms exist only when  $(m+n)$  is an odd integer. Table 1 shows values of the relative amplitude of the harmonics in the limiter output (Eq. (23)) for a partial set of values of  $m$  and  $n$ , where the two sine waves are 1 kc and 1.001 kc and  $a = 1$ . The power spectrum is plotted in Fig. 4.

2. General Case:  $V_1 > V_2$

In the general case for  $V_1 > V_2$  we have by Sonine and Schafheitlin (5c)

$$\int_0^{\infty} \frac{J_{\mu}(at) J_{\nu}(bt)}{t} dt = \frac{b^{\nu} \Gamma\left(\frac{\mu}{2} + \frac{\nu}{2}\right)}{2a^{\nu} \Gamma(\nu + 1) \Gamma\left(1 + \frac{\mu}{2} - \frac{\nu}{2}\right)} {}_2F_1\left(\frac{\mu + \nu}{2}, \frac{\nu - \mu}{2}; \nu + 1; \frac{b^2}{2a^2}\right) \quad (24)$$

for  $a > b$ . Substituting this in Eq. (21) we obtain the final result

$$y = \frac{a}{4\pi} \sum_{m=0}^{\infty} \sum_{n=0}^{\infty} \mathcal{E}_m \mathcal{E}_n [1 - (-1)^{m+n}] \frac{\lambda^n \Gamma\left(\frac{m+n}{2}\right)}{\Gamma(n+1) \Gamma\left(1 + \frac{m-n}{2}\right)} \sin \frac{(m+n)\pi}{2} \\ \times {}_2F_1\left(\frac{m+n}{2}, \frac{n-m}{2}; n+1; \lambda^2\right) [ \cos (m\omega_1 + n\omega_2)t + \cos (m\omega_1 - n\omega_2)t ], \quad (25)$$

where  $\lambda = (V_2/V_1) < 1$  and

$${}_2F_1(a, b; c; z) = 1 + \frac{ab}{c} \frac{z}{1!} + \frac{a(a+1)b(b+1)}{c(c+1)} \frac{z^2}{2!} + \dots$$

We note that this does not hold for the limiting case  $V_1 = V_2$ . In order to obtain an idea of how this function looks we plot (Fig. 5) the relative power output at the two fundamental frequencies as a function of the parameter  $x$  where  $V_1/V_2 = x/(1-x)$ . For  $x = 0$  or  $1$ , the single signal case is obtained. As  $x \rightarrow 0.5$ , the previous  $V_1 = V_2$  case is approached.

Table 1  
 Partial List of  $m$  and  $n$  Values Used to Evaluate  
 the Output of a Limiter (Eq. (23)) for the Special  
 Case  $V_1 = V_2 = V$ ;  $m + n = \text{Odd Integer}$ ;  $a = 1$

$m$	$n$	Output Frequency	Relative Amplitude	Output Power
5	4	996	0.090	0.008
4	3	997	-0.116	0.013
3	2	998	0.162	0.026
2	1	999	-0.270	0.073
1	0	1000	0.811	0.658
0	1	1001	0.811	0.658
1	2	1002	-0.270	0.073
2	3	1003	0.162	0.026
3	4	1004	-0.116	0.013
4	5	1005	0.090	0.008
3	0	3000	0.090	0.008
2	1	3001	-0.270	0.073
1	2	3002	-0.270	0.073
0	3	3003	0.090	0.008
4	1	5001	-0.054	0.003
3	2	5002	0.162	0.026
2	3	5003	0.162	0.026
1	4	5004	-0.054	0.003

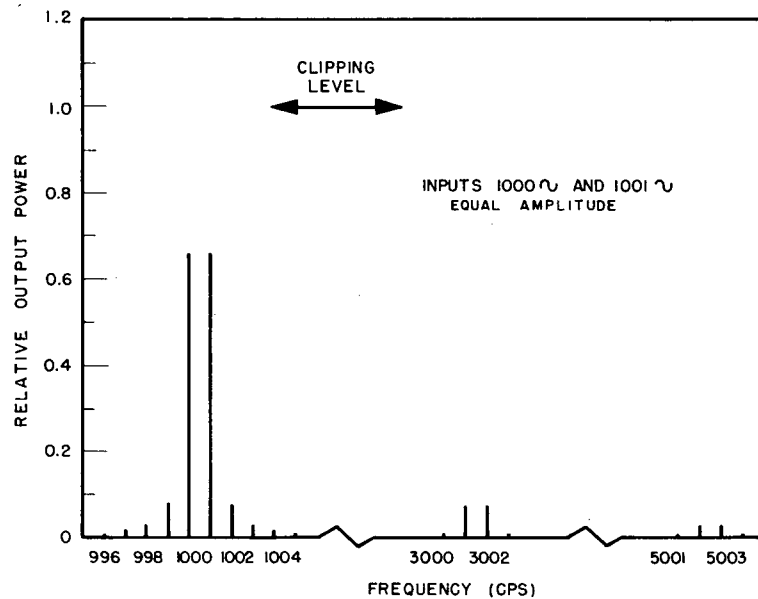


Fig. 4 - Output power spectrum of ideal limiter for input consisting of two sine waves of equal amplitude

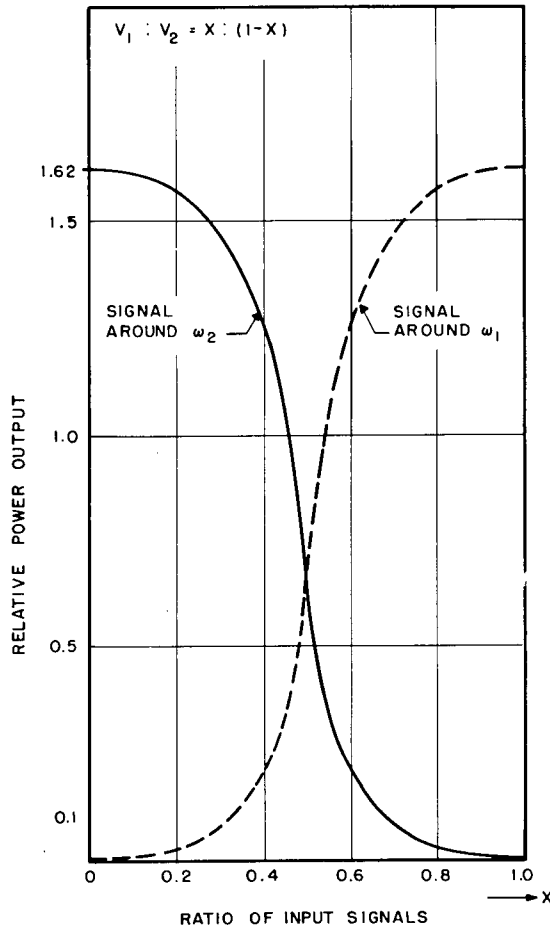


Fig. 5 - Power output at two fundamental frequencies for input consisting of two sine waves with varying amplitude ratio

In Fig. 6 the full spectrum is shown for the case  $\lambda = 0.5$  ( $x = 0.333$ ). Table 2 tabulates these results. Comparing Figs. 4 and 6, and also in Fig. 5, we note the strong attenuation effect of the ideal limiter on the weaker of two signals.

## PART II. NOISE ALONE

The general method of dealing with random noise is to use the Fourier cosine transform. Given an input power spectrum  $G(\omega)$ , the correlation function  $R(\tau)$  is the Fourier transform of  $G(\omega)$  given by

$$R(\tau) = \int_0^{\infty} G(\omega) \cos \omega\tau \, d\omega \quad (26)$$

where  $\tau$  is the time delay. The normalized correlation function is

$$\rho(\tau) = \frac{R(\tau)}{R(0)} \quad (27)$$

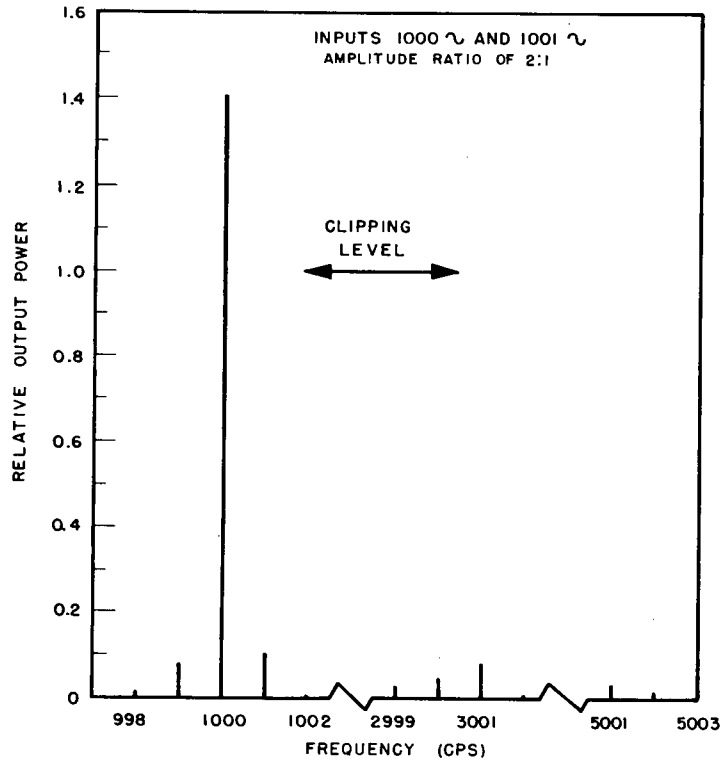


Fig. 6 - Output power spectrum of ideal limiter for input consisting of two sine waves of unequal amplitude

Table 2

Partial List of  $m$  and  $n$  Values Used to Evaluate the Output of a Limiter (Eq. (25)) for the Special Case  $v_1 = 2v_2$ , or  $\lambda = 0.5$ ;  $m + n = \text{Odd Integer}$ ;  $a = 1$

$m$	$n$	Output Frequency	Relative Amplitude	Output Power
3	2	998	0.106	0.011
2	1	999	-0.287	0.082
1	0	1000	1.189	1.414
0	1	1001	0.329	0.108
1	2	1002	-0.0426	0.002
4	1	2999	-0.181	0.033
3	0	3000	-0.208	0.043
2	1	3001	-0.287	0.082
1	2	3002	-0.0426	0.002
5	0	5000	-0.0212	0.000
4	1	5001	0.181	0.033
3	2	5002	0.106	0.011

The correlation function of the output is then (4)

$$a^2 \frac{2}{\pi} \sin^{-1} \{ \rho(\tau) \}, \quad (28)$$

and the output is the inverse transform of this

$$E(\omega) = \frac{4}{\pi^2} a^2 \int_0^\infty \sin^{-1} \{ \rho(\tau) \} \cos \omega \tau \, d\tau. \quad (29)$$

To evaluate this integral we have expanded

$$\sin^{-1} x = x + \frac{x^3}{6} + \frac{3x^5}{40} + \dots$$

#### Input of Band-Limited White Noise

The first case is band-limited white noise with infinitely steep skirts. This is an ideal, theoretical case which cannot be achieved in practice. The input is a constant amplitude distribution of frequencies over a given range (Fig. 7).

$$G(\omega) = \frac{K}{2\omega_a}, \quad \omega_0 - \omega_a < \omega < \omega_0 + \omega_a. \quad (30)$$

We are considering the special case where  $\omega_0$ , the center frequency, is three times  $\omega_a$ , the half-power frequency. In this case the Fourier transform of the input  $G(\omega)$  is

$$\begin{aligned} R(\tau) &= \frac{K}{2\omega_a} \int_{\omega_0 - \omega_a}^{\omega_0 + \omega_a} \cos \omega \tau \, d\omega \\ &= K \frac{\sin \omega_a \tau}{\omega_a \tau} \cos \omega_0 \tau, \end{aligned}$$

and

$$R(0) = K,$$

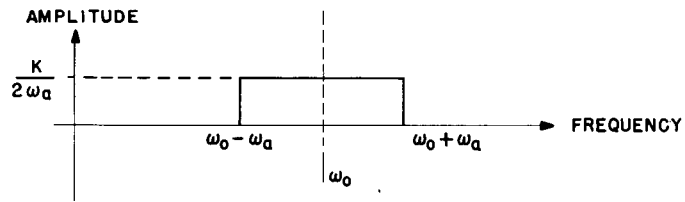
so

$$\rho(\tau) = \frac{\sin \omega_a \tau}{\omega_a \tau} \cos \omega_0 \tau. \quad (31)$$

The output power spectrum is then

$$E(\omega) = \frac{4}{\pi^2} \int_0^\infty \cos \omega \tau \sin^{-1} \left\{ \frac{\sin \omega_a \tau}{\omega_a \tau} \cos \omega_0 \tau \right\} d\tau. \quad (32)$$

Fig. 7 - Illustration of ideal, band-limited white noise with infinitely steep skirts



Expanding the  $\sin^{-1}$ , the first term will be

$$\begin{aligned} & \frac{4}{\pi^2} \int_0^\infty \cos \omega \tau \frac{\sin \omega_a \tau}{\omega_a \tau} d\tau \\ &= \frac{2}{\pi^2} \int_0^\infty \cos (\omega - \omega_0) \tau \frac{\sin \omega_a \tau}{\omega_a \tau} d\tau + \frac{2}{\pi^2} \int_0^\infty \cos (\omega + \omega_0) \tau \frac{\sin \omega_a \tau}{\omega_a \tau} d\tau \\ &= I_1 + I_2 . \end{aligned}$$

These integrals can each be expanded using  $2 \sin A \cos B = \sin (A+B) + \sin (A-B)$ . The second integral  $I_2$  is found to be zero. For  $I_1$  we have

$$I_1 = \begin{cases} 0 , & \omega < \omega_0 - \omega_a \\ \frac{1}{\pi \omega_a} , & \omega_0 - \omega_a < \omega < \omega_0 + \omega_a \\ 0 , & \omega_0 + \omega_a < \omega . \end{cases} \quad (33)$$

The first term of the output is plotted in Fig. 8. The second term can be calculated by similar methods and is found also to have no dc component (that is,  $E(\omega) = 0$  for  $\omega = 0$ ). The first two terms are plotted in Fig. 9. The maximum contribution of the second term is about 1/10 of the first. The third term is found to be about 1/10 the second. The second term also has a second peak at  $3\omega_0$ . The third term has a dc component which is about  $6 \times 10^{-4}$  times the peak value of the first term. In the more usual case where  $\omega_0 \gg \omega_a$ , dc components do not appear until much later terms and are negligibly small.

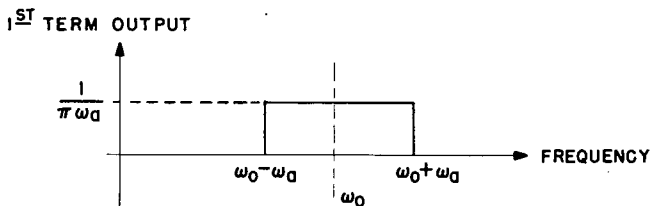


Fig. 8 - Plot of the first term in the equation for the power output spectrum of the band-limited white noise

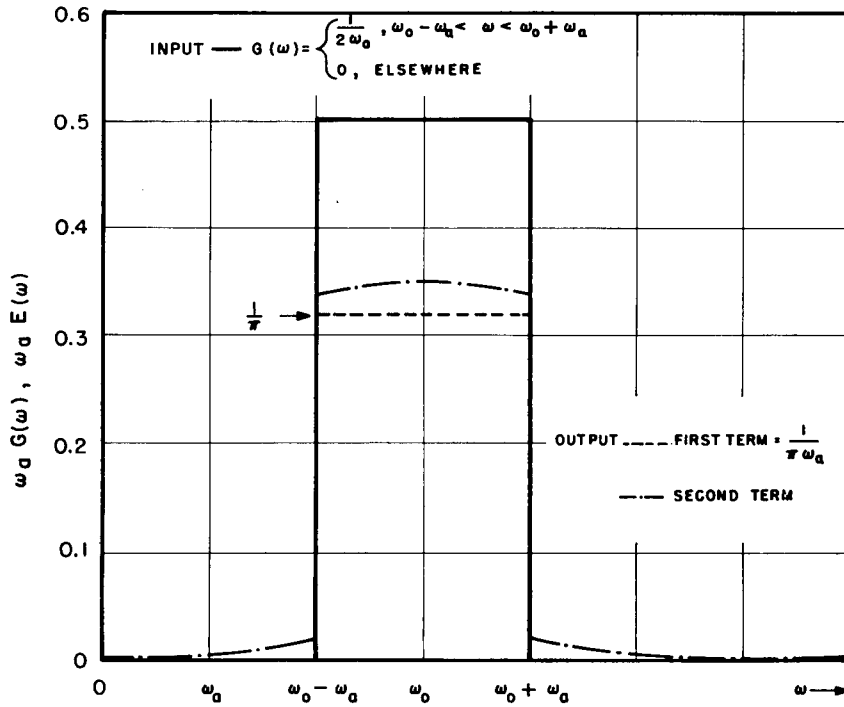


Fig. 9 - Effect of ideal limiting on the spectrum of band-limited white noise with infinitely steep skirts

#### White Noise Through Single-Tuned Circuit

As a second case of noise input we will consider the input represented by

$$G(\omega) = \frac{K}{1 + \left(\frac{\omega - \omega_0}{\omega_a}\right)^2} + \frac{K}{1 + \left(\frac{\omega + \omega_0}{\omega_a}\right)^2} \quad (34)$$

which could result from passing white noise through a single-tuned circuit. Here  $\omega_0$  is the center frequency and  $\omega_a$  is the half-bandwidth. We find

$$R(\tau) = K \omega_a \pi e^{-\omega_a |\tau|} \cos \omega_0 \tau$$

and

$$\rho(\tau) = e^{-\omega_a |\tau|} \cos \omega_0 \tau. \quad (35)$$

The power-spectrum output from an ideal limiter is then

$$E(\omega) = \frac{4}{\pi^2} \int_0^{\infty} \cos \omega \tau \sin^{-1} \left\{ e^{-\omega_a |\tau|} \cos \omega_0 \tau \right\} d\tau. \quad (36)$$

Using the first three terms of the  $\sin^{-1}$  expansion this integral was reduced to integrals of the form

$$\int_0^{\infty} e^{-p\omega_a |\tau|} \cos(\omega - q\omega_0)\tau \, d\tau$$

which were evaluated. Note that both input and output signals have a dc component (Figs. 10, 13, and 14).

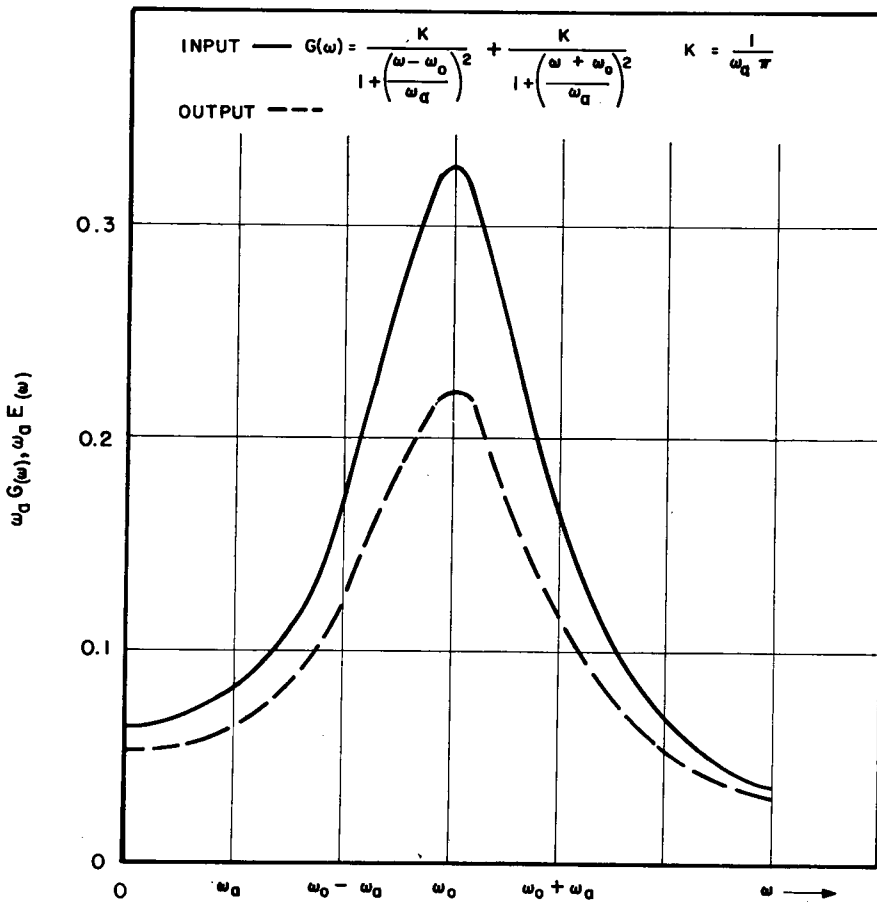


Fig. 10 - Effect of ideal limiting on the spectrum of white noise passed through a single-tuned circuit

**Bandpass Filter**

As the third case, consider three types of input noise provided by passing noise from some random source through a low-pass filter followed by a high-pass filter. The respective attenuations for these filters are given by

$$A = \left| \frac{Z_{in}}{Z_{out}} \right| = \left| \frac{1}{1 + j \left( \frac{\omega}{\omega_0} \right)} \right| = \frac{1}{\sqrt{1 + \left( \frac{\omega}{\omega_0} \right)^2}} ; \quad A' = \left| \frac{j \frac{\omega}{\omega_0}}{1 + j \left( \frac{\omega}{\omega_0} \right)} \right| = \frac{\left( \frac{\omega}{\omega_0} \right)}{\sqrt{1 + \left( \frac{\omega}{\omega_0} \right)^2}} \quad (37)$$

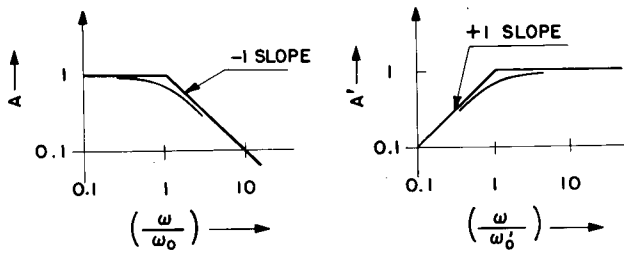


Fig. 11 - Illustration of the characteristics of a low-pass and a high-pass filter

The characteristics of these two filters are summarized in Fig. 11. Filters of this type are said to have a characteristic of  $\pm 1$  because of the slope of the asymptotes. When two filters follow each other (but are isolated to prevent interaction), the total attenuation is the product of the two attenuations. Letting  $\omega'_0 = n\omega_0$ , we have

$$A_T = AA' = \frac{\frac{\omega}{n\omega_0}}{\sqrt{1 + \left(\frac{\omega}{\omega_0}\right)^2} \sqrt{1 + \left(\frac{\omega}{n\omega_0}\right)^2}} \quad (38)$$

The power spectrum is

$$G(\omega) = A_T^2 = \frac{\left(\frac{\omega}{n\omega_0}\right)^2}{\left[1 + \left(\frac{\omega}{\omega_0}\right)^2\right] \left[1 + \left(\frac{\omega}{n\omega_0}\right)^2\right]} \quad (39)$$

Expanding this by partial fractions we get

$$G(\omega) = \frac{K}{1 + \left(\frac{\omega}{n\omega_0}\right)^2} - \frac{K}{1 + \left(\frac{\omega}{\omega_0}\right)^2} \quad (40)$$

where  $K$  is an amplification factor given by  $K = 1/(n^2 - 1)$ . Figure 12 shows the attenuation curve of this combination for  $n = 10$ .

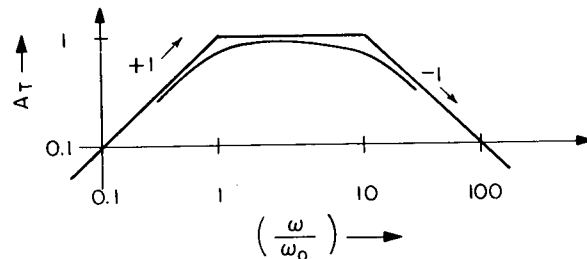


Fig. 12 - Attenuation curve for a high-pass and a low-pass filter in combination

Type 1: Choosing  $n = 10$  for  $G(\omega)$  (as above) we have

$$R(\tau) = K \frac{\pi}{2} \omega_0 \left[ 10 e^{-10 \omega_0 \tau} - e^{-\omega_0 \tau} \right]$$

$$\rho(\tau) = \frac{10}{9} e^{-10 \omega_0 \tau} - \frac{1}{9} e^{-\omega_0 \tau} \quad (41)$$

and

$$E(\omega) = \frac{4}{\pi^2} \int_0^{\infty} \cos \omega \tau \sin^{-1} \left\{ \frac{10}{9} e^{-10 \omega_0 \tau} - \frac{1}{9} e^{-\omega_0 \tau} \right\} d\tau. \quad (42)$$

We now expand the  $\sin^{-1}$ , producing integrals of the form

$$\int_0^{\infty} e^{-a\tau} \cos x\tau \, d\tau \quad \text{where } x = \omega/\omega_0.$$

While the input has no dc component, the output does have a dc component and is level over the low-frequency end up to about  $\omega/\omega_0 = 0.1$ . This filter-limiter system can provide constant-amplitude, white noise over the low-frequency end of the spectrum (see Figs. 13 and 14).\*

Type 2: As another case we take

$$G(\omega) = \left[ \frac{K}{1 + \left( \frac{\omega}{10 \omega_0} \right)^2} \right]^2 - \left[ \frac{K}{1 + \left( \frac{\omega}{\omega_0} \right)^2} \right]^2 \quad (43)$$

which may be thought of as an intermediate condition between the band-limited white noise and the previous case which had a characteristic of  $\pm 1$ . The characteristic of  $G(\omega)$  above is a band-pass filter with skirt asymptotes of  $\pm 2$ .

As before, we have

$$R(\tau) = \omega_0 \frac{\pi}{4} \left[ 10 (1 + \tau 10 \omega_0) e^{-10 \omega_0 \tau} - (1 + \tau \omega_0) e^{-\omega_0 \tau} \right]$$

$$\rho(\tau) = \frac{10}{9} (1 + 10 \omega_0 \tau) e^{-10 \omega_0 \tau} - \frac{1}{9} (1 + \omega_0 \tau) e^{-\omega_0 \tau} \quad (44)$$

and

$$E(\omega) = \frac{4}{\pi^2} \int_0^{\infty} \cos \omega \tau \sin^{-1} \left\{ \frac{10}{9} (1 + 10 \omega_0 \tau) e^{-10 \omega_0 \tau} - \frac{1}{9} (1 + \omega_0 \tau) e^{-\omega_0 \tau} \right\} d\tau. \quad (45)$$

Expanding the  $\sin^{-1}$  we get integrals of the same type as in the previous case and integrals of the form

$$\int_0^{\infty} \tau^n e^{-a\tau} \cos x\tau \, d\tau$$

which can be found in Bierens de Haan (7).

\*This effect was reported in "L. F. Random Signal Generator," J. L. Douce, and J. M. Shackleton, Electronic and Radio Engineering, August 1958, pp. 295-297.

Again, there is no dc component in the input. The output, normalized to have a peak value equal to the previous case, has a dc component, about 2.5 db lower, which is flat until  $\omega/\omega_0 = 0.02$ .

We see then that, as the skirts of the attenuation characteristic become steeper, the dc component of the output and the range over which it is flat decrease, the limiting case being the band-limited noise input (see Figs. 13 and 14).

Type 3: Finally we will consider the input

$$G(\omega) = \frac{K}{1 + \left(\frac{\omega}{2\omega_0}\right)^2} - \frac{K}{1 + \left(\frac{\omega}{\omega_0}\right)^2} \quad (46)$$

which is the same as type 1 except that now  $n = 2$ . We have

$$\begin{aligned} R(\tau) &= 2\omega_0 \frac{\pi}{2} e^{-2\omega_0\tau} - \omega_0 \frac{\pi}{2} e^{-\omega_0\tau} \\ \rho(\tau) &= 2e^{-2\omega_0\tau} - e^{-\omega_0\tau} \end{aligned} \quad (47)$$

and

$$E(\omega) = \frac{4}{\pi^2} \int_0^\infty \cos \omega\tau \sin^{-1} \left\{ 2e^{-2\omega_0\tau} - e^{-\omega_0\tau} \right\} d\tau \quad (48)$$

which we evaluate as before.

This result is essentially the same as type 1. The dc output level is slightly lower and the peak has moved to the right. The output is still flat within 1.5 db up to  $\omega/\omega_0 = 0.1$  (see Figs. 13 and 14).

In the following input and output spectrum plots, the input amplification constant  $K$  has been chosen to make  $\int_0^\infty G(\omega) d\omega = 1$  and, consequently,  $R(0) = 1$ . It should be noted that the total output power  $P_o$  is independent of the input power and depends only on the limiter voltage  $a$ ;  $P_o = \int_0^\infty E(\omega) d\omega = a^2$ . In the plots we have chosen  $a = 1$ . The inputs of the type

$$G(\omega) = \left[ \frac{1}{1 + \left(\frac{\omega}{n\omega_0}\right)} \right]^p - \left[ \frac{1}{1 + \frac{\omega}{\omega_0}} \right]^p$$

have been plotted in db (down from peak power) vs frequency. For  $p = 1$ ,

$$G(\omega)_{\max} = \frac{n-1}{n+1} \quad \text{and} \quad \frac{\omega}{\omega_0} = \sqrt{n}.$$

For  $p = 2$ , the expressions are more complicated; for  $n = 10$ ,  $G(\omega)_{\max} = 0.8847$  and  $\omega/\omega_0 = 1.954$ .

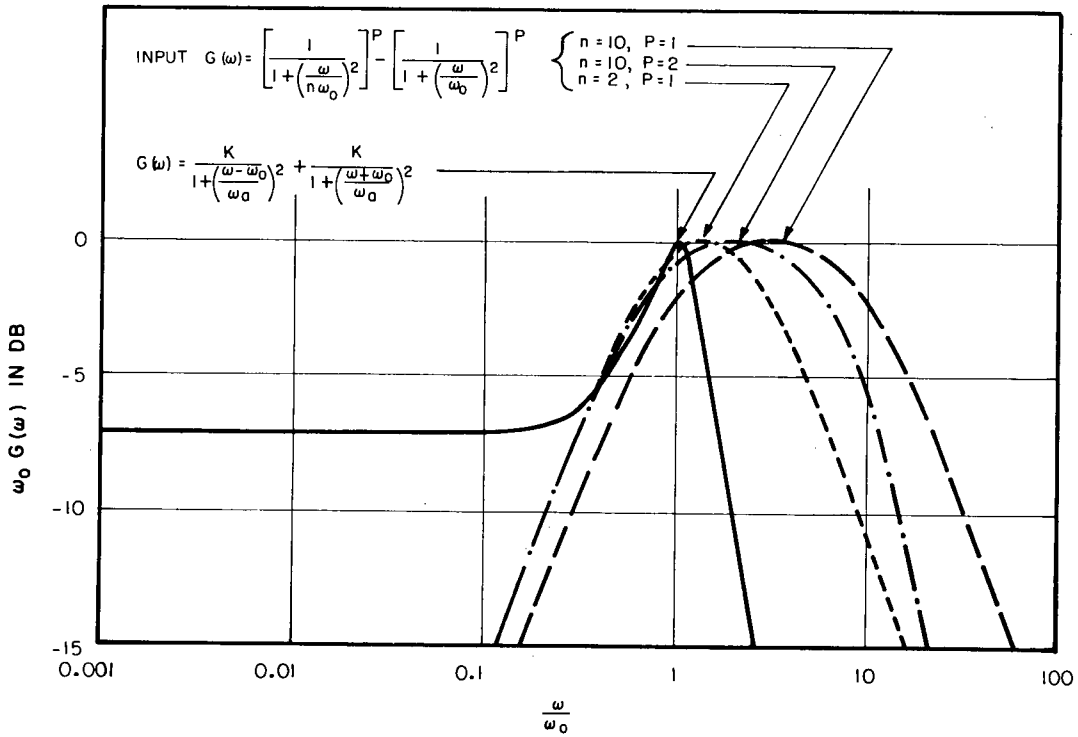


Fig. 13 - Input spectra of white noise passed through various band-pass filters

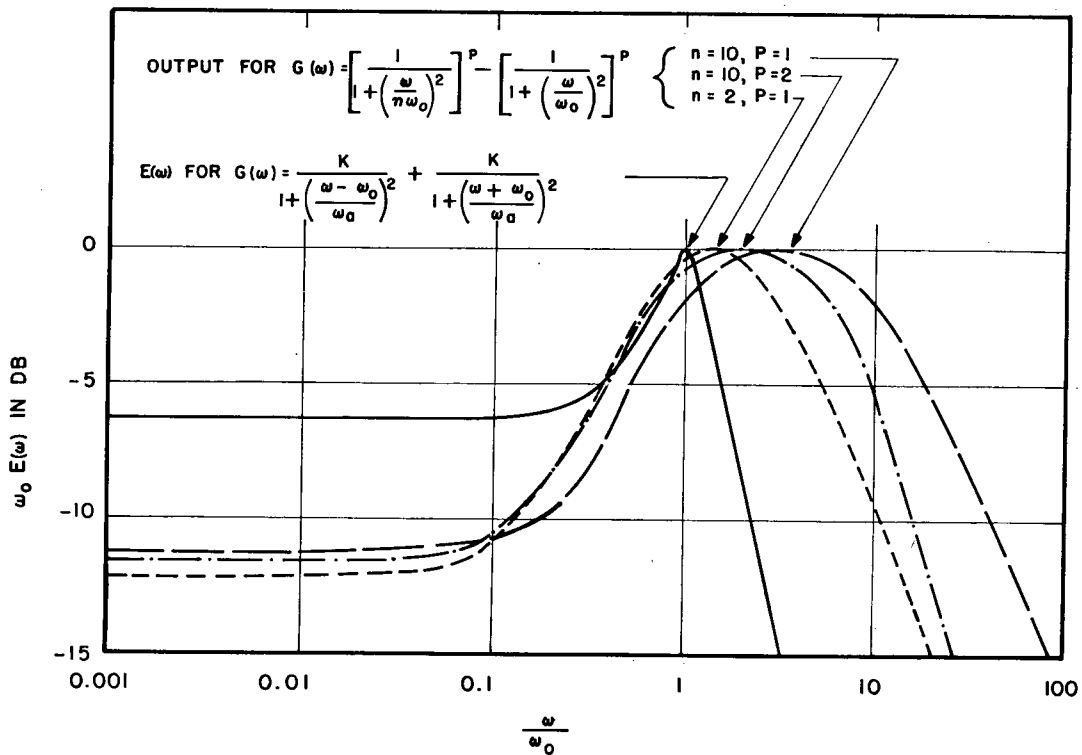


Fig. 14 - Output spectra after ideal limiting of band-pass filter inputs

## REFERENCES

1. Davenport, W.B., Jr., and Root, W.L., "An Introduction to the Theory of Random Signals and Noise," New York:McGraw-Hill (1958)
  - a. Chap. 13 on "The Transform Method," pp. 277-311
  - b. pp. 284-286
  - c. p. 285
2. Van Vleck, J.H., "The Spectrum of Clipped Noise," Harvard University Radio Research Lab. Report No. 51, July 21, 1943
3. Baum, R.F., "The Correlation Function of Smoothly Limited Gaussian Noise," IRE Transactions on Information Theory, Vol. IT-3, pp. 193-197, Sept. 1957
4. Lawson, J.L., and Uhlenbeck, G.E., "Threshold Signals," MIT Series, New York: McGraw-Hill, Vol. 24, pp. 57-58 (1950)
5. Watson, G.N., "A Treatise on the Theory of Bessel Functions," Cambridge: The University Press, 2nd ed. (1944)
  - a. p. 391
  - b. pp. 402-404, 13.41 (No. 7)
  - c. p. 401, 13.4(2)
6. Wylie, C.R., Jr., "Advanced Engineering Mathematics," New York:McGraw-Hill, 1st ed., p. 262 (1951)
7. Bierens de Haan, "Nouvelles Tables D' Intégrales Définies," New York:Strechert and Co., Table 361 (1939)

APPENDIX A  
EVALUATION OF CONTOUR INTEGRAL

From Eq. (19) of the text, the following contour integral must be evaluated

$$I = \int_{\epsilon - j\beta}^{\epsilon + j\beta} \frac{I_m(\omega V_1) I_n(\omega V_2)}{\omega} d\omega, \quad (A1)$$

over the contour shown in Fig. A1.

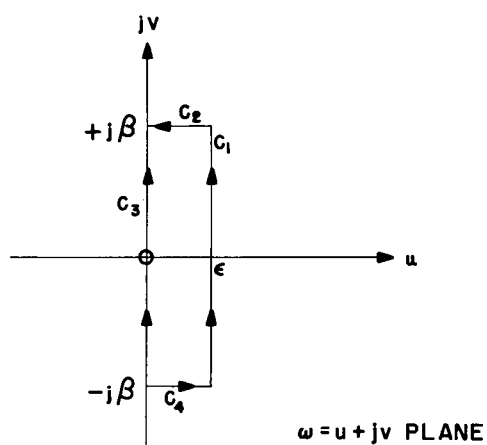


Fig. A1 - Contour integration paths for the evaluation of I in Eq. (A1)

For  $\omega = u + jv$ , let the contour integration be divided as follows:

$$\begin{aligned}
 I_1 &= \int_{\epsilon - j\beta}^{\epsilon + j\beta} \frac{I_m(\omega V_1) I_n(\omega V_2)}{\omega} d\omega, & \omega &= \epsilon + jv \\
 I_2 &= \int_{\epsilon + j\beta}^{-\epsilon + j\beta} \frac{I_m(\omega V_1) I_n(\omega V_2)}{\omega} d\omega, & \omega &= u + j\beta \\
 I_3 &= \int_{-\epsilon + j\beta}^{-\epsilon - j\beta} \frac{I_m(\omega V_1) I_n(\omega V_2)}{\omega} d\omega, & \omega &= jv \\
 I_4 &= \int_{-\epsilon - j\beta}^{\epsilon - j\beta} \frac{I_m(\omega V_1) I_n(\omega V_2)}{\omega} d\omega, & \omega &= u - j\beta \quad (A2)
 \end{aligned}$$

where  $I_1$  becomes  $I$  as  $\beta \rightarrow \infty$ . Now we have (6)

$$I_m(z) = \sum_{k=0}^{\infty} \left(\frac{z}{2}\right)^{m+2k} \frac{1}{k! \Gamma(m+k+1)}, \quad (\text{A3})$$

so that  $I_m(\omega V_1) I_n(\omega V_2)$  varies as  $\omega^{m+n}$  for small  $\omega$ . Since  $m$  and  $n$  cannot both be zero for our particular problem, the singularity in the integrand of  $I$  at the origin vanishes, and hence by Cauchy

$$I_1 + I_2 - I_3 + I_4 = 0. \quad (\text{A4})$$

To show that  $I_2 = 0$ , we first write  $I_m(z)$  for large  $|z|$  as (1c)

$$I_m(z) \doteq \frac{e^z}{\sqrt{2\pi z}}. \quad (\text{A5})$$

Along  $C_2$ ,  $\omega = u + j\beta$ , so for large  $\beta$  we find

$$I_2 = \int_{\epsilon + j\beta}^{j\beta} \frac{I_m(\omega V_1) I_n(\omega V_2)}{\omega} d\omega = \frac{e^{j\beta(V_1+V_2)}}{2\pi \sqrt{V_1 V_2}} \int_{\epsilon}^0 \frac{e^{u(V_1+V_2)}}{(u + j\beta)^2} du.$$

$$|I_2| \leq \frac{1}{2\pi \sqrt{V_1 V_2}} \int_{\epsilon}^0 \frac{e^{u(V_1+V_2)}}{u^2 + \beta^2} du \rightarrow 0 \quad \text{as } \beta \rightarrow \infty.$$

A similar argument shows  $I_4 = 0$ , and hence  $I_1 = I_3$ . Therefore, as  $\beta \rightarrow \infty$

$$I = \int_{-j\infty}^{j\infty} \frac{I_m(\omega V_1) I_n(\omega V_2)}{\omega} d\omega. \quad (\text{A6})$$

By letting  $\omega = jx$ , and recalling that  $I_m(jx) = j^m I_m(x)$ , we see that

$$\begin{aligned} I &= j^{m+n} \int_{-\infty}^0 \frac{J_m(xV_1) J_n(xV_2)}{x} dx + j^{m+n} \int_0^{\infty} \frac{I_m(xV_1) J_n(xV_2)}{x} dx \\ &= -j^{m+n} \int_0^{\infty} \frac{J_m(-xV_1) J_n(-xV_2)}{x} dx + j^{m+n} \int_0^{\infty} \frac{J_m(xV_1) J_n(xV_2)}{x} dx. \end{aligned}$$

But  $J_m(-x) = (-1)^m J_m(x)$ , and so, finally,

$$I = \int_{\epsilon - j\infty}^{\epsilon + j\infty} \frac{I_m(\omega V_1) I_n(\omega V_2)}{\omega} d\omega = j^{m+n} [1 - (-1)^{m+n}] \int_0^{\infty} \frac{J_m(xV_1) J_n(xV_2)}{x} dx.$$

## APPENDIX B

CALCULATION FOR THE CASE OF  
BAND-LIMITED WHITE NOISE

In the text we said that

$$E(\omega) = \frac{4}{\pi^2} \int_0^{\infty} \sin^{-1} \{ \rho(\tau) \} \cos \omega \tau \, d\tau \quad (\text{A7})$$

and the results of evaluating this integral were stated. As an example of the methods used we shall now perform the calculation for the case of band-limited white noise where

$$\rho(\tau) = \frac{\sin \omega_a \tau}{\omega_a \tau} \cos \omega_0 \tau. \quad (\text{A8})$$

We can write

$$E(\omega) = \sum_{k=1}^{\infty} T_k \quad \text{for } k \text{ odd} \quad (\text{A9})$$

where

$$T_k = \frac{4}{\pi^2} C_k \int_0^{\infty} \rho^k(\tau) \cos \omega \tau \, d\tau. \quad (\text{A10})$$

and

$$c_1 = 1, \quad c_3 = \frac{1}{6}, \quad c_5 = \frac{3}{40}, \quad \dots$$

We have first

$$T_1 = \frac{4}{\pi^2} \int_0^{\infty} \rho(\tau) \cos \omega \tau \, d\tau. \quad (\text{A11})$$

Using trigonometric identities

$$\begin{aligned} & \frac{\sin \omega_a \tau}{\omega_a \tau} \cos \omega_0 \tau \cos \omega \tau \\ &= \frac{1}{2} \frac{\sin \omega_a \tau}{\omega_a \tau} \{ \cos (\omega + \omega_0) \tau + \cos (\omega - \omega_0) \tau \} \\ &= \frac{1}{4 \omega_a} \{ \sin (\omega + \omega_0 + \omega_a) \tau - \sin (\omega + \omega_0 - \omega_a) \tau \\ & \quad + \sin (\omega - \omega_0 + \omega_a) \tau - \sin (\omega - \omega_0 - \omega_a) \tau \} \frac{1}{\tau}. \end{aligned} \quad (\text{A12})$$

Then,

$$T_1 = \frac{1}{\pi^2 \omega_a} \int_0^\infty \{\dots\} \frac{d\tau}{\tau}. \quad (\text{A13})$$

Now

$$\int_0^\infty \sin ax \frac{dx}{x} = \begin{cases} \frac{\pi}{2}, & a > 0 \\ -\frac{\pi}{2}, & a < 0 \end{cases}$$

so

$$T_1 = \frac{1}{\pi^2 \omega_a} \frac{\pi}{2} \begin{cases} +1, -1; & \omega + \omega_0 + \omega_a > 0, < 0 \\ -1, +1; & \omega + \omega_0 - \omega_a > 0, < 0 \\ +1, -1; & \omega - \omega_0 + \omega_a > 0, < 0 \\ -1, +1; & \omega - \omega_0 - \omega_a > 0, < 0 \end{cases} \quad (\text{A14})$$

which yields

$$T_1 = \begin{cases} \frac{1}{\pi \omega_a}, & \omega_0 - \omega_a < \omega < \omega_0 + \omega_a \\ 0, & \text{elsewhere.} \end{cases} \quad (\text{A15})$$